WORLD JOURNAL OF PHARMACEUTICAL RESEARCH
SJIF Impact Factor 8.084
Volume 12, Issue 20, 1023-1056. Research Article ISSN 2277–7105

INDOMETHACIN IN FOCUS: CHEMISTRY, PHARMACOKINETICS, AND ANALYTICS

Afzal Nagani*[1,2], Kripa Patel[1] and Moksh Shah[1]

[1]Parul Institute of Pharmacy, Parul University, Vadodara, 391760, Gujarat, India.

[2]Research and Development Cell, Parul University, Vadodara, 391760, Gujarat, India.

Article Received on
09 November 2023,

Accepted on 10 Nov. 2023

DOI: 10.20959/wjpr202320-30348

***Corresponding Author**
Afzal Nagani
Parul Institute of Pharmacy,
Parul University, Vadodara,
391760, Gujarat, India.

ABSTRACT

This article provides a comprehensive exploration of Indomethacin, a non-steroidal anti-inflammatory drug, from a chemistry perspective. It covers the drug's history, structural composition, mechanism of action, pharmacokinetics, adverse effects, contraindications, molecular docking study, and various analytical methods used for its determination. Indomethacin's synthesis and chemical characteristics are highlighted, making it a valuable resource for researchers, chemists, and healthcare professionals seeking a detailed understanding of this important pharmaceutical compound. The provided information discusses various aspects of Indomethacin, a non-steroidal anti-inflammatory drug. It covers the history, chemical structure, mechanism of action, pharmacokinetics, adverse effects, contraindications, and medical uses of Indomethacin. Molecular docking gives an idea about the binding affinity of indomethacin towards various protein structures; and shows binding affinity ranging from -6.5 kcal/mol to -9.6 kcal/mol, validation protocol, and method of docking also covered. Additionally, the article outlines numerous analytical methods for the determination of Indomethacin, including colorimetry, UV-Vis spectroscopy, fluorimetry, HPLC, LC-MS, and various electrochemical methods. The charts summarize the distribution of these analytical methods for Indomethacin determination.

Graphical Abstract

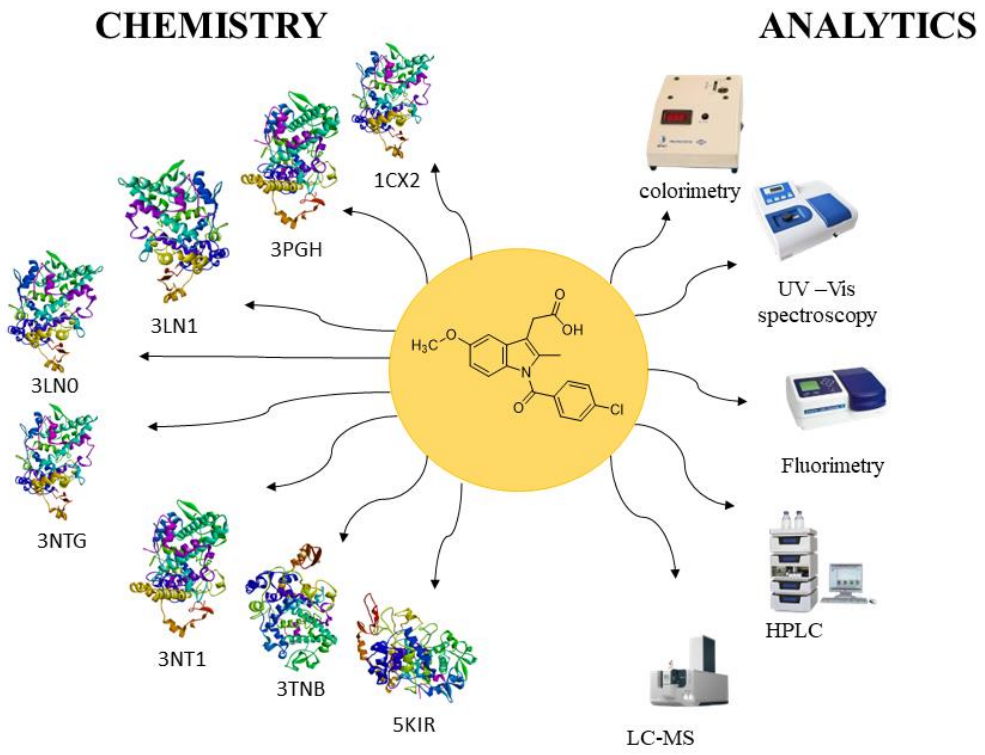

KEYWORDS: Molecular Docking, Indomethacin, UV-Vis spectroscopy, HPLC, LC-MS.

1. INTRODUCTION

1.1 Inflammation

1.1.1 The Latin verb "Inflammare," which meaning to burn, is where the word "inflammation" comes from. Any kind of injury to the human body has the potential to cause a number of chemical changes in the damaged area. At first, inflammation was thought to be a single illness resulting from abnormalities in body fluids. As far as current knowledge is concerned, inflammation is a normal reaction to a disruption or illness. Warmth, redness, swelling, discomfort, and decreased function are the main signs of inflammation. Generally speaking, inflammation is a continuum of stages that fall into three categories: the acute, transient phase, the delayed, sub-acute phase, and the chronic, proliferative phase. Increased vascular permeability causes inflammatory fluids to accumulate in the first phase, causing local edema. As the body's reaction to real or imagined injury, inflammation is typified by pain, warmth, redness, and swelling in the area that is impacted. Normally, inflammation functions as a defensive response, working to eliminate the initial agent of damage (toxins or bacteria) as well as the debris left behind by the injury (dead tissues and cells). However, if the inflammatory response is overstimulated or directed improperly, it can become harmful

on its own and cause organs, tissues, and cells to perish. Some of the most common and debilitating illnesses, including rheumatoid arthritis, Crohn's disease, lupus, psoriasis, asthma, and chronic bronchitis, are examples of such inappropriate or pathological inflammation.[3,65]

Inflammation is the natural defense mechanism of our bodies against tissue damage caused by physical injury, harmful chemicals, or microbial agents. This process involves a coordinated interplay of various factors that influence blood vessels, attract cells, and promote cell growth at different stages. Anti-inflammatory agents have multiple potential targets for interventions, but corticoids, such as glucocorticoids, are the most effective in suppressing the inflammatory response. However, it's important to note that corticoids only provide relief without addressing the root cause of inflammation, which means that the underlying condition persists, albeit with subdued symptoms. The use of corticoids can also lead to an increased susceptibility to infections due to the compromised microorganism-killing capacity of defensive cells. Additionally, they hinder the healing process and formation of scars, and in some cases, peptic ulcers may perforate without exhibiting symptoms. Therefore, caution must be exercised to avoid indiscriminate use of corticoids due to the potential risks involved.

In addition to corticosteroids, Non-Steroidal Anti-Inflammatory Drugs (NSAIDs) are also used to treat inflammation. NSAIDs work by inhibiting the production of prostaglandins (PGs) or specifically targeting cox-2. However, this inhibition of PG production can have negative effects like damage to the gastric mucosa, bleeding, and impaired platelet function. It can also cause delayed or prolonged labor, asthma, and anaphylactoid reactions in some people. Additionally, cox-2 inhibition may increase cardiovascular risks.

Inflammation is recognized as a fundamental physiological defense mechanism that enables the body to shield itself against infections, burns, toxic substances, allergens, and other harmful stimuli. When inflammation becomes uncontrolled and persistent, it can contribute as an underlying factor in many chronic illnesses.[67] Despite its protective function, the intricate processes and mediators involved in the inflammatory response can either trigger, sustain, or exacerbate various diseases (Sosa *et al.*, 2002). Currently available anti-inflammatory drugs are associated with significant side effects. Hence, there is a pressing need for the development of potent anti-inflammatory drugs with fewer adverse effects.

1.1.2 Causes

Burns, chemical irritants; frostbite, toxins; infection by pathogens; physical injury (blunt or penetrating); immune reactions due to hypersensitivity; ionizing radiation; trauma; foreign bodies, including splinters, dirt, and debris.

1.1.3 Types

There are two primary types of inflammation: acute and chronic. The body's first reaction to damaging stimuli is known as acute inflammation, which is characterized by an increased flow of plasma and specific white blood cell types—granulocytes in particular—from the bloodstream into the damaged tissues. This inflammatory response is further amplified and matured by a sequence of biochemical reactions that involve the immune system, the local vascular system, and different cells inside the damaged tissue. Chronic inflammation is defined as an extended period of inflammation that results in a progressive change in the cell composition at the site of inflammation. Because of the continuous inflammatory activity, it is characterized by a process of tissue destruction and healing occurring simultaneously.

Inflammation can be classified into two primary types - acute and chronic. The initial response of the body to injury or damage is known as acute inflammation. This response is characterized by an increased flow of plasma and specific white blood cell types, particularly granulocytes, from the bloodstream into the affected area. The immune system, the local vascular system, and different cells within the damaged tissue further amplify and mature this inflammatory response through a sequence of biochemical reactions. Chronic inflammation is defined as an extended period of inflammation that leads to a gradual change in the cellular composition of the affected area. This type of inflammation is characterized by continuous inflammatory activity and a process of tissue destruction.

Acute inflammation represents a natural and essential reaction by the body to any form of injury. Essentially, it occurs when the body's immune system ramps up its activity. Inflammation is the intricate biological process responsible for combatting potentially harmful conditions brought about by foreign organisms.

Table 1: Comparison between Acute and Chronic Inflammation.

Comparison between Acute and Chronic Inflammation		
Characteristics	**Acute**	**Chronic**
Causative agent	Bacterial Pathogens, injuredtissues	Persistent acute inflammationdue to non-degradable pathogens, viral infection, persistent foreign bodies, or autoimmune reactions
Major cells involved	Neutrophils are the primary responders, while eosinophils and basophils respond to helminth worms and parasites. Mononuclear cells, including monocytes and macrophages, are also involved in the response.	Mononuclear cells, including monocytes, macrophages, lymphocytes, and plasma cells, as well as fibroblasts, are all types of cells that are classified based on their nucleus structure. Mononuclear cells, including monocytes, macrophages, lymphocytes, and plasma cells, as well as fibroblasts, are all types of cells that are classified based on their nucleus structure.
Primary mediators	Vasoactive amines,eicosanoids	IFN-γ and other cytokines,growth factors, reactive oxygen species, hydrolyticenzymes
Onset	Immediate	Delayed
Duration	Few days	Up to many months, or years
Outcomes	olution, abscess formation,chronic inflammation	Tissue destruction, fibrosis,necrosis

2. Introduction to Indomethacin

2.1 History

Indomethacin, a non-steroidal anti-inflammatory drug, was uncovered and synthesized by the research team at Merck Sharp and Dohme Laboratories. This medication possesses the ability to reduce inflammation, lower fever, and provide pain relief. Indomethacin has proven to be a valuable treatment option for patients dealing with moderate to severe conditions such as rheumatoid arthritis, ankylosing spondylitis, osteoarthritis, acute painful shoulder (bursitis and/or tendinitis), and acute gouty arthritis. More recently, it has also demonstrated effectiveness in treating neonates with a patent ductus arteriosus and in patients experiencing acute cystoid macular edema following cataract surgery. Indomethacin is used worldwide and is available in various forms, including formulations designed for extended activity. The discovery of this compound has opened up new avenues for the medical management of debilitating diseases.[5]

2.2 Structural form

Indomethacin (abbreviated as INDO) is a compound derived from indole-acetic acid, specifically known as [1-(4-chlorobenzoyl)-5-methoxy-2-methylindol-3-yl] acetic acid. It was granted a patent in 1961 and received approval for medical use in 1963.[14,15] The structural representation of indomethacin is provided in **Scheme 1**.

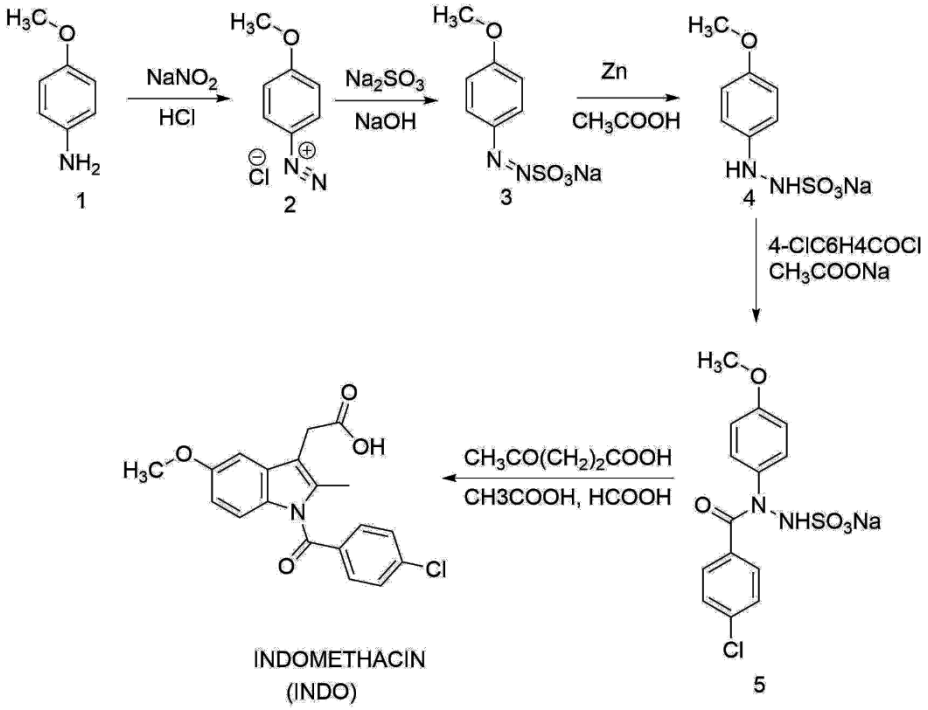

Scheme 1: Synthetic Procedure For Indomethacin.

In 2005, Magedov and his team developed a new method for producing a chemical compound called INDO. The process began with 4-methoxyaniline (1), which was then transformed into 4-methoxybenzenediazonium chloride (2) using diazotization. This was further converted into sodium 4-methoxybenzene-diazosulfonate (3), which was then transformed into sodium 2-(4-methoxyphenyl)-1-hydrazosulfonate (4) using zinc dust. The team then mixed compound 4 with 4-chlorobenzoyl chloride, creating sodium 2-(4-chlorobenzoyl)-2-(4-methoxyphenyl)-1-hydrazosulfonate (5).

The final step involved converting hydrazine 5 into INDO, but for this, an acidic substance was required that served two purposes. Firstly, it had to remove the sulfonate protection from the nitrogen atom, creating a hydrazone when combined with levulinic acid. Secondly, it had to catalyze the Fisher reaction without removing the 4-chlorobenzoyl group. The team achieved this using formic acid as the catalyst (see Scheme 1).

2.3 Mechanism of Action

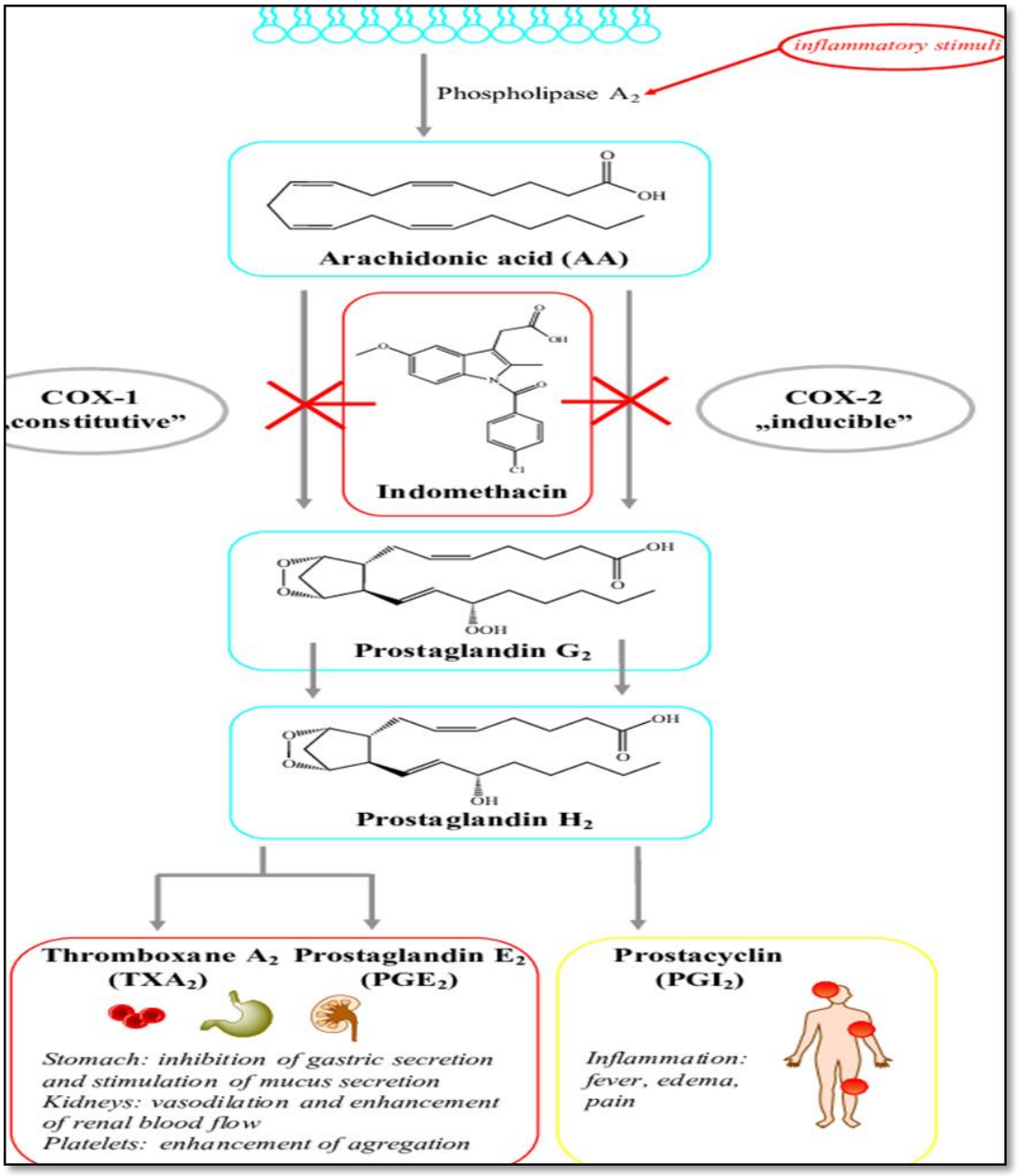

Figure: 1 Lipid Formulations and Bioconjugation Strategies for Indomethacin Therapeutic Advances - Scientific Figure on ResearchGate. Available from: https://www.researchgate.net/figure/The-mechanism-of-action-of-indomethacin_fig1_350069598 [accessed 28 Oct, 2023]

2.4 Pharmacokinetic characteristics

Orally, indomethacin is readily absorbed; however, its absorption through the rectal route is gradual but consistent. 90% of it is partially digested and 90% binds to plasma proteins in the liver to inactive substances and discharged via kidney. Plasma half-life is two to five hours.

Absorption: Indomethacin is efficiently absorbed, taking two hours to reach peak plasma concentrations. The bioavailability is over 100 percent.

Distribution: Indomethacin is easily able to pass across the blood-brain barrier due to its high lipid solubility. In synovial fluid, indomethacin likewise reaches a high concentration.

Metabolism: Indomethacin is metabolized by enterohepatic circulation. Demethylation and deacylation are the processes that break down indomethacin. O-desmethyl-indomethacin, O-deschlorobenzoyl-indomethacin, and their conjugates with glucuronides are the main metabolites.

Excretion: Renal tubular secretion excretes around 60% of the supplied indomethacin in urine, while biliary secretion excretes the remaining 40% in feces. Because of enterohepatic circulation, indomethacin's elimination half-life, which is roughly 7 hours, can vary greatly (1.5 to 16 hours).[1,2,3]

2.5 Adverse Effects

The most frequent side effects include nausea, dizziness, headaches, and dyspepsia. It is important to understand that indomethacin is used to treat a variety of headache conditions, and that headaches are among the most frequent side effects.[6]

Indomethacin has been known to trigger hypersensitivity events, such as urticaria, angioedema, and anaphylaxis. As was already noted, prostaglandins are produced by COX-1 to preserve the stomach mucosa, and indomethacin is a non-selective COX inhibitor. Constipation, diarrhoea, nausea, and dyspepsia (indigestion) can occur when this mechanism is inhibited. Peptic ulcer development, however, is the most serious adverse effect of indomethacin on the stomach. Depending on where they are located, peptic ulcers can cause mid-epigastric discomfort that is either eased or made worse by food. Similarly, gastric ulcers cause pain that is made worse by food.[7] Additionally, indomethacin can have an impact on the liver, leading to jaundice and increased liver enzymes.[8]

2.6 Contraindications

Pregnant women, children, drivers, people with mental health issues, epileptics, and those with kidney condition should not use it.[3] Because of prominent adverse effects, When more tolerable nonsteroidal anti-inflammatory drugs (NSAIDs) are not working to treat illnesses like ankylosing spondylitis, acute exacerbations of destructive arthropathies, psoriatic

arthritis, acute gout, or rheumatoid arthritis, indomethacin is used as a backup medication. When better-tolerated NSAIDs are not working to treat illnesses like ankylosing spondylitis, acute exacerbations of destructive arthropathies, psoriatic arthritis, acute gout, or rheumatoid arthritis, indomethacin is used as a stand-by medication. Indomethacin may help treat fever related to cancer that is resistant to other antipyretics. It has been the most widely used medication for the medical closure of patent ductus arteriosus; in most cases, closure is achieved with three 12-hour intravenous injections at a dose of 0.1–0.2 mg/kg. Bartter's syndrome exhibits a significant response to various inhibitors of PG production as well.[3]

2.7 Uses

Given its severe adverse effects, indomethacin is reserved for treatment in cases of severe rheumatoid arthritis, acute exacerbations of degenerative arthropathies, psoriatic arthritis, acute gout, or ankylosing spondylitis that do not respond to better-tolerated nonsteroidal anti-inflammatory medications. When various antipyretics fail to relieve a cancer-related fever, indomethacin may be able to assist. For the medical closure of patent ductus arteriosus, it has been the most commonly utilized medicine; three 12-hour intravenous injections at a dose of 0.1–0.2 mg/kg are typically required to accomplish closure. Additionally, a notable response to several PG synthesis inhibitors is seen in Bartter's syndrome.[3]

3 MATERIALS AND METHODS

3.1 Selection of Ligand

With the aid of Discovery Studio 2021, ligand was generated for validation purposes. In this co-crystal ligand was isolated from deleting protein and preserved as lignad.mol2 was then opened in AutoDockTools-1.5.6 ligand to give them torsion before being finally saved as pdbqt. Additionally, indomethacin was made with ChemDraw 21.0.0, and energy was reduced with Chem3D 21.0.0. **FIGURE-2** mentions co-crystal ligands.

3.2 Selection of Protein

The crystallographic structure of COX2 and indomethacin is available under Code ID 4COX (Mus musculus) at 2.90 (Å).[68] Additionally, COX2 is complexed with SC-558 and flurbiprofen under code 1CX2, 3PGH (Mus musculus) with resolutions of 3.00 (Å) and 2.50 (Å) respectively.[69] The crystal structures of Celecoxib, 5c-S, SC-75416, 23d-(R) are available under Code ID 3LN1, 3LN0, 3MQE, 3NTG (Mus musculus) with resolutions of 2.40 (Å), 2.20 (Å), 2.80 (Å), and 2.19 (Å) respectively.[70] The structures of Naproxen and 6-methylthio naproxen are available under Code ID 3NT1 and 3NTB (Mus musculus) with

resolutions of 1.73 (Å) and 2.23 (Å) respectively.[71] Finally, the crystal structure of Rofecoxib is available under Code ID 5KIR (Homo sapiens) with a resolution of 2.70 (Å).[72] All of these structures can be obtained from the online Protein Data Bank (PDB) (https://www.rcsb.org/).

3.3 Computation preparation

3.3.1 Preparation of ligand

Here, we used Indomethacin as a standard inhibitor. The 2D structure of indomethacin was drawn by ChemDraw 21.0.0 software and this was further converted into the 3D structure with the help of Chem3D 21.0.0, which was used for converting indomethacin to its three-dimensional structure. Indomethacin was optimized by energy minimization using the MM2 method[73] by using a short key (Ctrl + M) and saved in mol2 format.[74]

3.3.2 Preparation of Protein

Here, we used various protein structures as mentioned above. The general procedure for the preparation of protein is, In the first step downloaded protein was opened in Discovery Studio 2021 Client (Accelrys lnc, San Diego, CA, USA). after that choose Receptor – Ligand Interaction module then select inbuilt ligands like indomethacin, SC-558, flurbiprofen, for 4COX, 1CX2, 3PGH (Mus musculus) (Kurumbail et al. 1996) respectively, Celecoxib, 5c-S, SC-75416, 23d-(R) for 3LN1, 3LN0, 3MQE, 3NTG (Mus musculus)[70] respectively and for 5KIR (Homo sapiens)[72] Rofecoxib. Attributes were copied from that and pasted at the configuration file after that deleted this inbuilt ligand and save file in the format of Protein Data Bank (.pdb). after this AutoDockTools-1.5.6[75] was used for converting pdb to pdbqt format. For that in the first step water was removed and polar hydrogen and Kollman charges were added. After that, it was shaved in (.pdbqt) format.

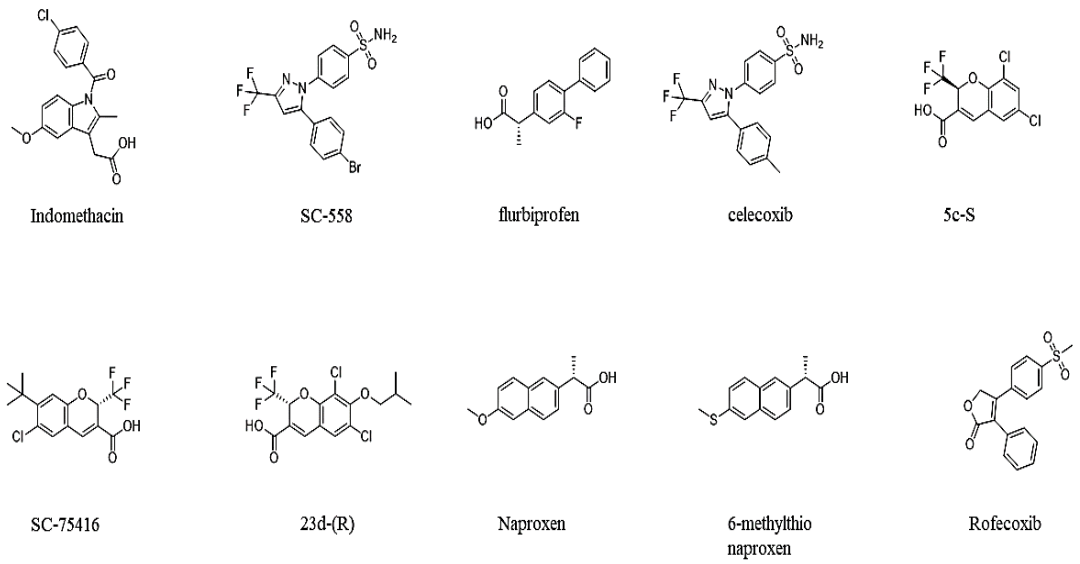

Figure 2: Co crystal ligand of various PDB ID's.

3.4 Docking Study

Molecular docking was performed to investigate how the indomethacin could potentially bind to the active sites of the target PDBs, using AutoDock Vina 1.5.6.[75]

3.4.1.1 General Process for Validation and Docking

The protein was subjected to a validation process involving several steps. Initially, the ligand was removed from the protein structure and prepared for the docking study, and save in the format of mol2. After that with the help of AutoDockTools-1.5.6[75] conversion of the structure into a pdbqt extension file for we were performed a few steps, in fist step ligand was opened in ADT after that went to Ligand → Torsion Tree → Choose Root → Detect Root → Aromatic Carbon → Aromaticity Criterion here Cutoff Angle must be 7.5 → Output → save as Ligand. pdbqt. Subsequently, additional preparations were made for the protein, the all-inbuilt ligand molecules were deleted after that save in the form of Protein.pdb this much preparation was done by Discovery Studio 2021 Client (Accelrys lnc, San Diego, CA, USA). further preparations were carried out for the protein in ADT. These included removing water molecules, adding polar hydrogen, and assigning Kollman charges after that go to Grid → macromolecule → Choose → Protein → Select molecule → "-contains no non-bonded atoms" This message shown then click ok after this protein was automatically saved inside the directory folder. Now for grid generation original downloaded protein data bank file was loaded to Discovery studio 2021 Client after that we selected the inbuilt ligand where we were supposed to bind our targeted molecule then right clicked → Attributes of ligand →

copy XYZ → pasted it to the configuration file, the format for configuration file was mentioned **FIGURE:3** saved it config.txt by named.

```
receptor = 4COX.pdbqt
ligand = Ligand.pdbqt

center_x = 24.7
center_y = 22.33
center_z = 15.23

size_x = 40
size_y = 40
size_z = 40

out = OUTPUT.pdbqt

exhaustiveness = 8
```

Figure 3: Configuration file.

To run Autodock Vina The script was downloaded from (https://vina.scripps.edu/downloads/) then we went to This PC→ Program file (×86) → The Scripps Research Institute → Vina → copied all three files and pasted into a working folder. After that, The AutoDock Tool Vina was run via the command prompt using the following command.

"vina.exe --config conf.txt --log log.txt"

This Docked conformer and previously saved ligand in the form of .pdbqt both were opened in Discovery studio 2021 Client and RMDS was calculated. For RMSD we performed the following steps Loaded both ligands → select standard ligand → structure → RMSD → set reference, then again followed till four steps, and then last, we clicked on Heavy atoms. RMSD was automatically calculated.

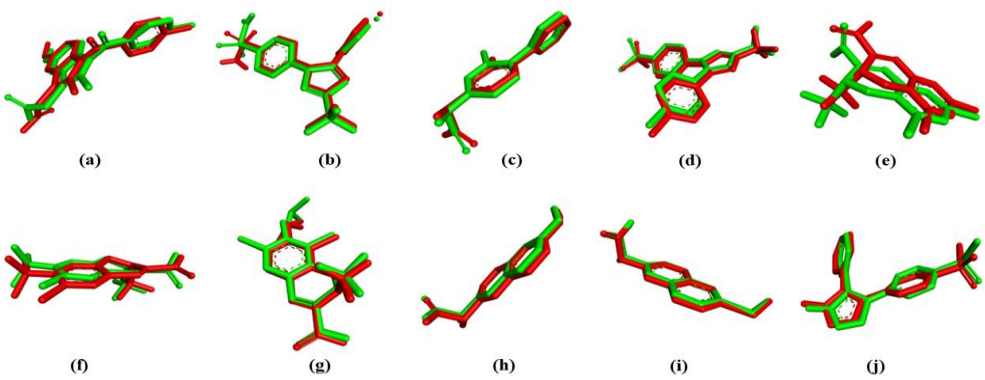

Figure 4: Using AutoDock software, the binding mode of a potent COX-2 inhibitor was validated.: in red, the crystallographic pose; in green, the top-ranked docking

solution.[a] Indomethacin (PDB ID 4COX); [b] SC-558 (PDB ID 1CX2), [c] flurbiprofen (PDB ID 3PGH); [d] celecoxib (PDB ID 3LN1); [e] 5c-S (PDB ID 3LN0); [f] SC-75416 (PDB ID 3MQE); [g] 23d-(R) (PDB ID 3NTG); [h] Naproxen (PDB ID 3NT1); [i] 6-methylthio naproxen (PDB ID 3NTB); (j) Rofecoxib (PDB ID 5KIR).

Table 2: shows the validation results of all test protein.

Receptor Ligand	**RMSD (Å)**	**Affinity (kcal/mol)**	**IC50 (nM)**	**Amino acid residues**	**Grid box coordinate (size) X Y Z**	**Grid box size (Å)**
4COX Indomethacin	0.882	-10.6	0.48[68]	120-Arg, 355-Tyr, 349-Val, 523-Val, 527-Ala, 385-Tyr, 387-Trp, 384-Leu, 90-His, 522-Met	Center_ 24.848720 22.294640 15.125640	40 × 40 × 40
1CX2 SC-558	0.827	-11.0	9.3[69]	120-Arg, 355-Tyr, 359-Leu, 349-Val, 523-Val, 353-Ser, 527-Ala, 526-Gly, 385-Tyr, 387-Trp, 381-Phe, 384-Leu, 90-His, 352-Leu, 513-Arg, 518-Phe	Center_ 24.263071 21.528071 16.496500	40 × 40 × 40
3PGH flurbiprofen	0.390	-8.9	10[69]	120-Arg, 352-Leu, 349-Val, 527-Ala, 355-Tyr, 531-Leu	Center_ 25.712056 22.225056 15.052389	30 × 30 × 30
3LN1 celecoxib	0.873	-12.3	0.07[70]	31Tyr, 345-Leu, 509-Val, 339-Sser, 513-Ala, 371-Tyr, 373-Trp, 370-Leu, 499-Arg, 75-His, 504-Phe	Center_ 30.988577 -22.283615 -16.507231	40 × 40 × 40
3LN0 5c-S	1.086	-9.3	9.8[70]	335-Val, 341-Tyr, 513-Ser, 509-Val, 512-Gly, 508-Met, 338-Leu, 371-Tyr, 504-Phe, 516-Ser	Center_ 26.556211 23.798000 15.337789	40 × 40 × 40
3MQE SC-75416	1.2113	-9.1	5.0[70]	513-Ala, 335-Val, 341-Tyr, 509Val, 508-Met, 371-Tyr, 512-Gly.	Center_ 19.954773 -16.345545 -59.329318	30 × 30 × 30
3NTG	0.8089	-10.0	28[70]	371-Tyr, 373-Trp,	Center_	30 ×

23d-(R)				338-Leu, 509-Val, 513-Ala, 335-Val, 504-Phe, 106-Arg, 517-Leu, 345-Leu.	26.728500 21.487542 17.161375	30 × 30
3NT1 Naproxen	0.3611	-9.2	60[71]	120-Arg- 355-Tyr, 531-Leu, 527-Ala, 349-Val, 526-Gly, 352-Leu, 385-Tyr, 523-Val, 387-Trp.	Center_ -40.698706 -51.500412 -22.399706	30 × 30 × 30
3NTB 6-methylthio naproxen	0.2744	-8.8	670[71]	120-Arg- 355-Tyr, 531-Leu, 527-Ala, 349-Val, 526-Gly, 352-Leu, 385-Tyr, 523-Val, 387-Trp, 381-Phe.	Center_ -58.677412 45.111000 -15.411529	30 × 30 × 30
5KIR Rofecoxib	0.9017	-10.2	1[72]	518-Phe, 517-Ile, 90-His, 192-Gln, 352-Leu, 527-Ala, 349-Val, 355-Tyr, 523-Val, 353-Ser.	Center_ 23.206000 1.318136 34.258864	30 × 30 × 30

3.4.1.2 General Process for Docking of Indomethacin

Indomethacin was prepared as we mentioned earlier in the Preparation of ligand, this prepared ligand was loaded to the ADT and the same procedure was followed which we had mentioned in the general process for validation. and for protein, the validated protein was simply copied to a working folder. and configuration file also copied. Then to run AutoDock Vina simple command was used. The docking result, including binding affinities (Kcal/mol) for indomethacin, were recorded. And interaction was visualized by Discovery Studio 2021 Client.

Table 3: shows Docking result of indomethacin in all protein.

Receptor	Affinity (kcal/mol)	Amino acid residues
4COX[68]	-8.4	120-Arg, 524-Glu, 523-Val, 90-His, 89-Val, 100-Trp, 93-Leu, 112-Ile, 119-Ser.
1CX2[68]	-8.0	120-Arg, 359-Leu, 116-Val, 531-Leu, 527-Ala, 349-Val, 352-Leu, 522-Mat, 518-Phe, 387-Trp, 523-Val, 513-Arg, 355-Tyr.
3PGH[68]	-8.0	120-Arg, 123-Leu, 524-Glu, 523-Val, 90-His, 355-Tyr, 89-Val, 115-Tyr.
3LN1[69]	-9.2	513-Ala, 517-Leu, 345-Leu, 99-Met, 102-Val, 373-Trp, 371-Tyr, 338-Leu, 509-Val, 504-Phe, 75-His, 341-Tyr, 339-Ser.
3LN0[69]	-6.5	341-Tyr, 355-Val, 345-Leu, 102-Val, 99-Met, 517-Leu, 513-Ala, 371-Tyr, 373-Trp, 338-Leu, 509-Val, 75-His.

3MEQ[70]	-8.3	106-Arg, 517-leu, 513-Ala, 509-Val, 499-Arg, 338-Leu, 335-Val, 371-Tyr, 75-His, 102-Val.
3NTG[70]	-7.2	106-Arg, 105-Ser, 101Tyr, 74-Val, 341-Tyr, 78-Leu, 102-Val, 77-Ile, 98-Ile, 85-Trp.
3NT1[71]	-8.0	120-Arg, 523-Val, 355-Tyr, 86-Pro, 83-Lys, 119-Ser, 89-Val, 93-Leu, 116-Val, 112-Ile, 100-Trp.
3NTB[71]	-7.8	120-Arg, 89-Val, 90-His, 123-Leu, 524-Glu.
5KIR[72]	-9.6	120-Arg, 527-Ala, 349-Val, 355-Ryr, 531-Leu, 359-Leu, 110-Val, 387-Trp, 523-Val, 518-Phe, 352-Leu, 192-Gln.

3.5 ADMET Calculation

The introduction of a drug molecule to the market is contingent upon both its efficacy and safety. Analyzing its absorption, distribution, metabolism, excretion, and toxicity (ADMET) profile is one way to look at these characteristics.[76, 84] ADMET properties of indomethacin was estimated by online SwissADME (http://www.swissadme.ch/) server listed in Table – 3.

The input section of the SwissADME server includes a molecular sketcher that uses Marvin, a JavaScript program from Chemaxon (https://chemaxon.com/). With this program, users can import, sketch, and edit 2D chemical structures, then turn them into a list of molecules. Additionally, SMILES notation can be entered into the structure through editing in a conventional text format. The screened structure is assessed for a number of factors, such as absorption properties, toxicity, and interactions with metabolizing enzymes.[77]

Table 4: The ADMET properties of indomethacin was computed by Swiss ADME.

GI Absorption	BBB	P-gp substrate	CYP1A2 inhibitor	CYP2C19 inhibitor	CYP2C9 inhibitor	CYP2D6 inhibitor	CYP3A4 inhibitor	Log k_p cm/s
High	Yes	No	Yes	Yes	Yes	No	No	-5.45

3.6 Rule of five

The flexibility, molecular size, and hydrophobicity of a compound can significantly influence how it behaves within a living organism. Achieving optimal bioavailability requires striking a suitable equilibrium between permeability and solubility characteristics.[78] The evolution of molecular characteristics of compound was conducted using the Molinspiration online server, accessible at (https://www.molinspiration.com/).

Table 5: The molecular properties of indomethacin was computed using Molinspiration.

miLogP	TPSA	nAtoms	MW	nON	nOHNH	nRotb	nviolation
3.99	68.54	25	357.79	5	1	4	0

3.7 RESULT AND DISCUSSION

3.7.1 Docking simulation study

The original crystallographic structure of the COX-2 inhibitor indomethacin was matched with the molecular superposition approach to validate its validity (PDB ID 4COX/ Mus musculus), SC-558 (PDB ID 1CX2/ Mus musculus), flurbiprofen (PDB ID 3PGH/ Mus musculus), celecoxib (PDB ID 3LN1/ Mus musculus), 5c-S (PDB ID 3LN0/ Mus musculus), SC-75416 (PDB ID 3MQE/ Mus musculus), 23d-(R) (PDB ID 3NTG/ Mus musculus), Naproxen (PDB ID 3NT1/ Mus musculus), 6-methylthio naproxen (PDB ID 3NTB/ Mus musculus) and Rofecoxib (PDB ID 5KIR/ Mus musculus) the best classified slot position obtained were compared. The outcomes, depicted in **FIGURE-4**, illustrate the alignment of the suggested binding modes for our inhibitors within the active site of COX-2 (refer to **FIGURE-4**). The superposition results in an overlap RMSD of 0.882 (Å) for indomethacin (PDB ID 4COX), 0.827 (Å) for SC-558 Å (PDB ID 1CX2). 0.390 (Å) for flurbiprofen (PDB ID 3PGH), 0.873 (Å) for celecoxib (PDB ID 3LN1), 1.086 (Å) for 5c-S (PDB ID 3LN0), 1.211 (Å) for SC-75416 (PDB ID 3MQE), 0.80 (Å) for 23d-(R) (PDB ID 3NTG), 0.361 (Å) for naproxen (PDB ID 3NT1), 0.274 (Å) for 6-methylthionaproxen (PDB ID 3NTB) and 0.901 (Å) for Rofecoxib (PDB ID 5KIR). These measurements fall below the widely accepted tolerance threshold of 2.0 (Å), as documented by[79] and[80] This affirms the validation of our molecular docking process.[81]

The binding affinities of indomethacin with different protein ID can be compared (see the **TABLE-3**). The standard indomethacin structure shows binding affinity -8.4 (kcal/mol) with in 4COX PDB ID with amino acid interactions like 120-Arg, 524-Glu, 523-Val, 90-His, 89-Val, 100-Trp, 93-Leu, 112-Ile, 119-Ser. This same compound shows binding affinity -8.0 (kcal/mol), -8.0 (kcal/mol), -9.2 (kcal/mol), -6.5 (kcal/mol), -8.3 (kcal/mol), -7.2 (kcal/mol), -8.0 (kcal/mol), -7.8 (kcal/mol), -9.6 (kcal/mol) with in PDB ID 1CX2, 3PGH, 3LN1, 2LN0, 3MQE, 3NTG, 3NT1, 3NTB, SKIR respectively.

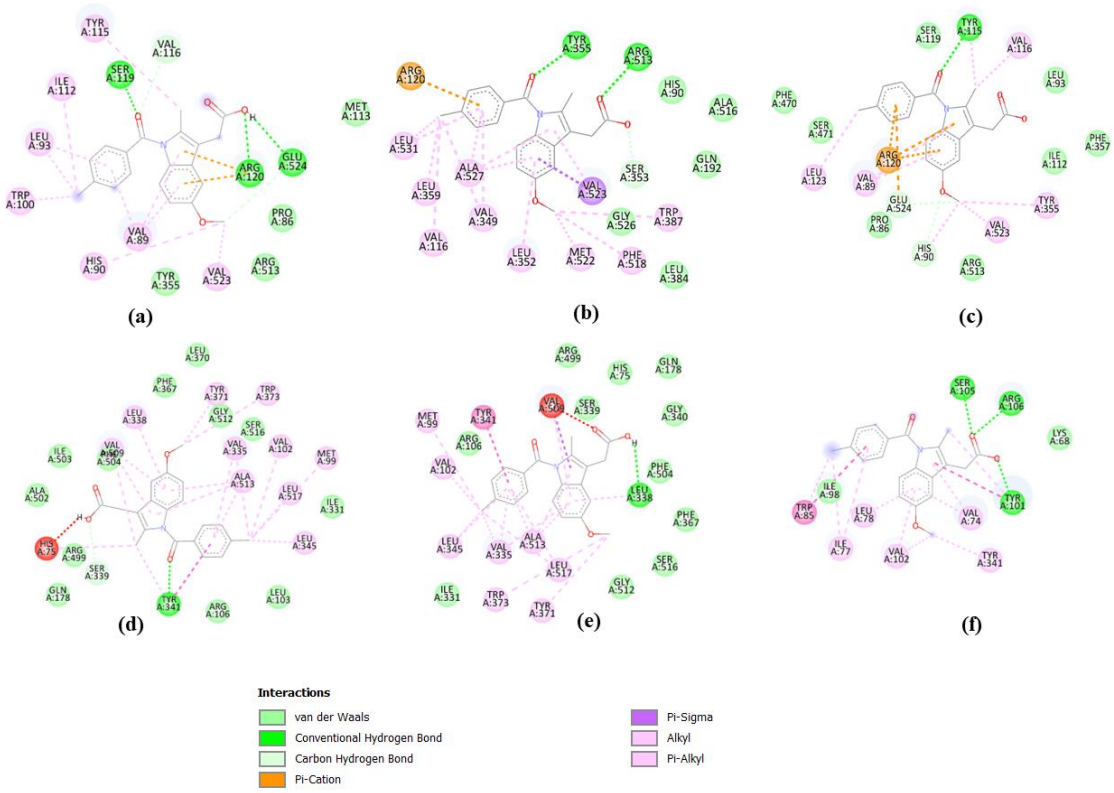

FIGURE:5 Best binding pose and interaction of indomethacin in various Protein (a) PDB ID 4COX; (b) PDB ID 1CX2; (c) PDB ID 3PGH; (d) PDB ID 3LN1; (e) PDB ID 3LN0; (f) PDB ID 3MEQ.

Interaction similarity % of Indomethacin with compared to the co crystal ligand SC-558 for PDB ID 1CX2 was found to be 76.92% with the common interactions 120-Arg, 359-Leu, 527-Ala, 349-Val, 352-Leu, 518-Phe, 387-Trp, 523-Val, 513-Arg, 355-Tyr. Indomethacin shows common interactions 513-Ala, 345-Leu, 373-Trp, 371-Tyr, 509-Val, 504-Phe, 75-His, 339-Ser comparison with celecoxib with in PDB ID 3LN1.Futhermore 341-Tyr, 355-Val, 371-Tyr, 338-Leu, 509-Val interactions were found in PDB ID 3LN0 with compared to 5c-S. Other interactions for difference PDB IDs were mentioned in **TABLE - 3**.

Indomethacin shows Salt Bridge interaction as 120-Arg with -OH group of carboxylic acid, π-Sigma interaction with indole moiety as 527-Ala, 349-Val, 523-Val. -OCH_3 group shows two types of interaction which are π- alkyl and Carbon Hydrogen bond with 90-His and 352-Leu respectively. Halogen atom of molecule which show various π-alkyl interactions with 384-Leu, 522-Met, 381-Phe, 387-Trp. Benzene rig which shows π-π shaped interaction with 385-Tyr. Oxygen of carbonyl group which shows Conventional Hydrogen Bond within PDB ID 4COX.[68]

In PDB ID 1CX2 indole ring of indomethacin shows π-Sigma interaction with 523-Val and pi-Alkyl interactions with 527-Ala and 352-Leu, benzene ring shows maximum pi-Alkyl interactions with 359-Leu, 531-Leu, 116-Val, 349-Val and important interaction as pi-Cation with 120-Arg. Other interactions are 355-Tyr and 513-Arg as Conventional Hydrogen Bond. (see **FIGURE:5**)

Within PDB ID 3PGH indole ring if indomethacin shows π-Cation interaction with 120-Arg and pi-sigma interaction with 89-Val. -OCH_3 group which show Alkyl interaction with 355-Tyr, 90-His, 523-Val. Other interactions are 123-leu, 155-Tyr. (See **FIGURE:5**)

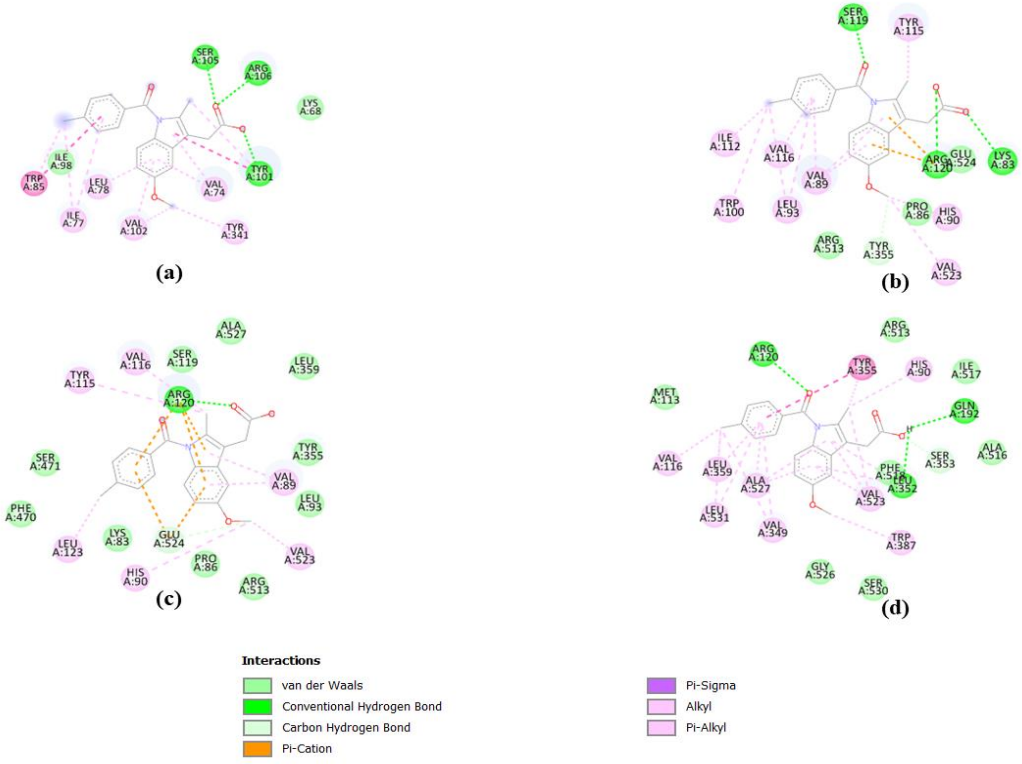

Figure 6: Best binding pose and interaction of indomethacin in various Protein (a) PDB ID 3NTG; (b) PDB ID 3NT1; (c) PDB ID 3NTB, (d) PDB ID 5KIR.

Indomethacin shows good binding affinity and interaction with Protein structure under PDB ID 3LN1 4 Methoxy substitution on benzene ring shows pi- Alkyl interactions with 345-Leu, 102-Val, 99-Met, 517-Leu, 335-Val. Carbonyl oxygen which shows Conventional Hydrogen Bond With 341-Tyr. (see **FIGURE:5**)

Furthermore 341-Tyr, 355-Val, 371-Tyr, 338-Leu, 509-Val interactions were found in PDB ID 3LN0 with compared to 5c-S. In PDB ID 3MEQ 106-Arg, 517-leu, 513-Ala, 509-Val,

499-Arg, 338-Leu, 335-Val, 371-Tyr, 75-His, 102-Val interaction was observed in which 513-Ala, 335-Val, 371-Tyr are the similar to the co crystal ligand SC-75416. In PDB ID 3NTG one common interaction was observed that is 106-Arg. Important interaction 120-Arg was observed in the PDB ID 3NT1 and other interactions were 523-Val, 355-Tyr, 86-Pro, 83-Lys, 119-Ser, 89-Val, 93-Leu, 116-Val, 112-Ile, 100-Trp observed. Indomethacin that shows two common interactions in both PDB ID 3NT1 and 3NTB was 120-Arg and 89-Val. It was observed that indomethacin that show interaction in the COX-1 PDB ID 5KIR also which are 120-Arg, 355-tyr, 531-Leu, 527-Ala.

Indomethacin interaction with other protein structure under different PDB IDs and shows different types of interaction as mention above **TABLE-3**. Most of this interaction which match with the interaction of inbuilt co crystal ligand see **TABLE-2**. 2D representation of interaction of indomethacin (see **FIGURE:6**).

3.7.2 ADMET Study

ADMET characteristics play a crucial role in identifying and developing potential therapies. The probability of clinical success can be increased by selecting drug candidates based on both pharmacological properties and ADMET screening. The ADMET parameters of the indomethacin compound were estimated using the SwissADME servers.[82] Crucial physicochemical, pharmacokinetic, and drug-related parameters are offered by this freely accessible web tool. These include drug-likeness, lipophilicity, solubility, pKa, permeability, absorption, bioavailability, penetration of the blood-brain barrier, interactions with transporters, penetration of the skin and eyes, binding of plasma proteins, metabolic processes, drug-drug interactions, volume of distribution, clearance, and half-life for one or more molecules. Crucial physicochemical, pharmacokinetic, and drug-related parameters are offered by this freely accessible web tool. These include drug-likeness, lipophilicity, solubility, pKa, permeability, absorption, bioavailability, penetration of the blood-brain barrier, interactions with transporters, penetration of the skin and eyes, binding of plasma proteins, metabolic processes, drug-drug interactions, One or more molecules were analyzed for their volume of distribution, clearance, and half-life. The SwissADME web tool was used to thoroughly investigate the parameters, including the impact of the compounds on p-glycoprotein efflux and inhibition, as well as cytochrome P450 (CYP450) enzymes. It is worth noting that all parameters were thoroughly analyzed.[83] ADMET result of indomethacin is shown in **TABLE-4**.

3.7.3 Rule of Five

During the study of indomethacin, Lipinski's rule of five was applied. The molinspiration server was used to calculate additional physical and chemical features of the substance.[78] To determine the hydrogen bonding capability, the number of nitrogen and oxygen atoms in the chemical structure was taken into account. Moreover, the TPSA, which is the surface area covered by polar atoms, and the count of rotatable bonds were also computed for the candidate compounds. See **TABLE-5.**

4. Analytical methods for the determination of 'INDOMETHACIN'

Table-6.

METHOD	SAMPLE	CONDITIONS AND CHARACTERISTIC METHOD PARAMETERS	REFERENCE
Colorimetry	INDO Capsules	Max. Absorption: 470 Nm; Temperature: 30°C (5 Min), 50°C (20 Min); And Solvent: Glacial Acetic Acid	[9]
UV-Vis Spectroscopy	Pharm. Prep.	Max. Absorption: 510 Nm; Temperature: 30°C; And Solvent: Naoh (1 M)	[10]
UV-Vis Spectroscopy	Pharm. Prep.	Max. Absorption: 284.65 Nm; Solvent: Methanol	[11]
UV-Vis Spectroscopy	Pharm. Prep.	Max. Absorption: 320 Nm; Solvent: Methanol; And Hydrotropic Agent: Niacinamide (2 M)	[12]
UV-Vis Spectroscopy	Pharm. Prep.	Max. Absorption: 228 Nm And Solvent: KOH (0.1 M)	[13]
UV-Vis Spectroscopy	Pharm. Prep.	Max. Absorption: 235 Nm And Solvent: Naoh (0.1 M)	[14]
UV-Vis Spectroscopy	Pharm. Prep.	Max. Absorption: 320 Nm And Hydrotropic Mixture: Sodium Caprylate (10%), Sodium Benzoate (10%), And Niacinamide (10%)	[15]
UV-Vis Spectroscopy	Pharm. Prep.	Max. Absorption: 320 Nm And Hydrotropic Mixture: Sodium Acetate (5%), Sodium Citrate (5%), And Urea (10%)	[16]
UV-Vis Spectroscopy	Pharm. Prep.	Max. Absorption: 266 Nm And Solvent: Ethanol (50%)	[17]
UV-Vis Spectroscopy	Pharm. Prep.	Max. Absorption: 319 Nm And Solvent: Naoh (0.5 M)	[18]
Fluorimetry Combined With SIA	Pharm. Prep.	Solvent: Naoh (0.1 M) And Hexadecyltrimethylammonium Bromide (20 Mm); FR: 0.8 Ml·Min−1; Ex: 278 Nm, Em: 358 Nm	[19]
Fluorimetry Combined With SIA	Human Urine, Pharm. Prep.	Solvent: Methanol (40%); FR: 1.5 Ml·Min−1; Ex: 283 Nm, Em: 371 Nm	[20]
Fluorimetry Combined With SIA	Pharm. Prep.	Solvent: Methanol And Phosphate Buffer (Ph 7.2); FR: 1.0 Ml·Min−1; Ex: 278 Nm, Em: 378 Nm	[21]

Fluorimetry Combined With FIA	Pharm. Prep.	Solvent: Naoh (0.1 M); FR: 1.7 Ml·Min−1; Ex: 184.9 Nm, Em: 253.7 Nm	[22]
Phosphorimetry	Pure INDO Solution	Solvent: Naoh (0.05 M); Ex: 297 Nm, Em: 450 Nm	[23]
Chemiluminescence	Human Urine	Solvent: Hcl (0.1 M); MIP Column: 15 Mm × 4 Mm; Monomer: Methacrylic Acid; Adsorption Time: 50 S, FR: 1.5 Ml·Min−1, Washing Time: 80 S With Formaldehyde; Reaction Time: 30 S	[24]
Chemiluminescence Combined With SIA	Pharm. Prep.	Solvent: Ethanol (50%); FR: 100 Ml·S−1 (Detection), 60 Ml·S−1 (Aspiration); Aspirated Solution: Ce(Iv) (15 Mm) In H2SO4 (50 Mm), Tris(2,2′-Bipyridyl) Ruthenium(Ii) (0.5 Mm), And Sodium Acetate (0.4 M), INDO	[25]
Chemiluminescence	Water Samples, Human Plasma	Solution: Sulfur And Nitrogen Codoped Carbon Quantum Dots, H_3PO_4 (4 M), INDO, And $Kmno_4$ (5×10^{-5} M)	[26]

Table-7.

METHOD	SAMPLE	CONDITIONS AND CHARACTERISTIC METHOD PARAMETERS	REFERENCE
GC–MS	Human Serum And Plasma	Solvent: Methanol; MP: Nitrogen; Column Pressure: 34473.79 Pa; Column: Zebron ZB-1 (15 M × 0.25 Mm × 0.25 µm); T R: 8.8 Min; Vaporization Temperature: 40°C; Electron Impact Mode, 280°C	[27]
HPLC (Equine serum)	Equine Serum	Solvent: Methanol; MP: Acetonitrile–Water (51:49); FR: 1 Ml·Min−1; Column: C18, Beckman (250 Mm × 4.6 Mm) With 5 µm Particles; T R: 13.4 Min; UV Detection (254 Nm)	[28]
HPLC (Pharm. prep.)	Pharm. Prep.	Solvent: Methanol; MP: Acetonitrile–Phosphoric Acid (50:50); FR: 0.6, 1.2 Ml·Min−1; Columns: Zorbax SB-Phenyl (75 Mm × 4.6 Mm) With 3.5 µm Particles And Zorbax SB-CN (150 Mm × 4.6 Mm) With 5 µm Particles; T R: 3.6 Min; UV Detection (237 Nm)	[29]
HPLC (Porcine plasma)	Porcine Plasma	Solvent: Methanol; MP: 60% Acetonitrile In 0.02 M Sodium Acetate Buffer, Adjusted To Ph 3.6 Using Orthophosphoric Acid; FR: 1 Ml·Min−1; Column: C18 Res Elut Reversed-Phase Column (150 Mm × 4.6 Mm) With 5 µm Particles; T R: 3.6 Min; UV Detection (320 Nm)	[30]
HPLC (Plasma of premature neonates)	Plasma Of Premature Neonates	Solvent: Methanol; MP: Methanol–Water–Orthophosphoric Acid (70:29.5:0.5); FR: 1.5 Ml·Min−1; Column: Hypersil ODS C18 Column (125 Mm × 4 Mm) With 5 µm Particles; T R: 2.9 Min; UV Detection (270 Nm)	[31]
HPLC (Human urine,	Human Urine, Pharm. Prep.	Solvent: Methanol; MP: Methanol–Water–Acetic Acid (67:33:0.1); FR: 1 Ml·Min−1; Column:	[32]

Pharm. prep.)		Nucleosil RP-C18 (250 Mm × 4.6 Mm) With 5 µm Particles; T R: 7.2 Min; Chemiluminescence Detection	
HPLC (Human plasma)	Human Plasma	Solvent: Ethanol (96%); MP: Acetonitrile–Water (63:37), Adjusted To Ph 2 With Orthophosphoric Acid; FR: 0.8 Ml·Min−1; Column: Silica Gel Column Prodigy RP C18 (150 Mm × 4.6 Mm) With 5 µm Particles, Equipped With 0.5 Mm Prefilter And A Guard Column ODS C18; T R: 6.27 Min; UV Detection (270 Nm)	[33]
HPLC (Pharm. prep.)	Pharm. Prep.	Solvent: MP; MP: Orthophosphoric Acid–Methanol–Acetonitrile (40:20:40); FR: 2 Ml·Min−1; Column: Lichrosorb C18 (250 Mm × 4.6 Mm) With 5 µm Particles; T R: 7.42 Min; UV Detection (240 Nm)	[34]
HPLC (Pharm. prep.)	Pharm. Prep.	Solvent: Methanol; MP: Sodium Phosphate Buffer, Ph 7.0 And Acetonitrile (35:75); FR: 1 Ml·Min−1; Column: Lichrosorb C8 (250 Mm × 4.6 Mm) With 5 µm Particles; T R: 6.96 Min; UV Detection (230 Nm)	[35]
HPLC (Rabbit blood plasma)	Rabbit Blood Plasma	Solvent: Methanol; MP: 0.8 Ml Phosphoric Acid Mixed With 600 Ml Methanol And Volume Made Up To 1,000 Ml With Water; FR: 1.5 Ml·Min−1; Column: Hypersil BDS C18 (250 Mm × 4.6 Mm) With 5 µm Particles; T R: 13.83 Min; UV Detection (240 Nm)	[36]
HPLC (Pharm. prep.)	Pharm. Prep.	Solvent: MP; MP: Ethyl Acetate; FR: 1 Ml·Min−1; Column: Lichrosphere RP C8 (250 Mm × 4 Mm) With 5 µm Particles; T R: 2.44 Min; UV Detection (318 Nm)	[37]
HPLC (Pharm. prep.)	Pharm. Prep.	Solvent: Methanol; MP: Methanol–Orthophosphoric Acid (70:30); FR: 1.5 Ml·Min−1; Column: Luna C18 (2) 100 R (250 Mm × 4.6 Mm) With 5 µm Particles; T R: 11.29 Min; UV Detection (254 Nm)	[38]
HPLC (Rabbit plasma)	Rabbit Plasma	Solvent: MP; MP: Acetonitrile–Phosphate Buffer, Ph 4.6 (35:65); FR: 1 Ml·Min−1; Column: Kromosil C18 (250 Mm × 4.6 Mm) With 5 µm Particles; T R: 3.31 Min; UV Detection (260 Nm)	[39]
HPLC (Human serum and plasma)	Human Serum And Plasma	Solvent: Methanol; MP: Methanol–Water (Gradient), Ph 4.5; FR: 1 Ml·Min−1; Column: C18 (250 Mm × 4.6 Mm) With 5 Mm Particles; T R: <3.5 Min; UV Detection (254 Nm)	[40]
HPLC (Pure mixture of drugs)	Pure Mixture Of Drugs	Solvent: Methanol; MP: Acetonitrile-Phosphate Buffer (65:35); FR: 1 Ml·Min−1; Column: Gemini RP-C18 Column (250 Mm × 4.6 Mm) With 5 µm Particles Equipped With Gemini C18 Precolumn; Room Temperature; UV Detection (320 Nm)	[41]
HPLC (Pharm. prep.)	Pharm. Prep.	Solvent: Methanol; MP: Methanol–Acetonitrile–Sodium Acetate Buffer Ph 3 (10:50:40); FR: 1 Ml·Min−1; Column: Zorbax Eclipse Plus C18	[42]

		(100 Mm × 4.6 Mm) With 3.5 µm Particles; T R: 3.767 Min; UV Photo Diode Array Detection (254 Nm)	
HPLC (Pharm. prep.)	Pharm. Prep.	Solvent: Methanol; MP: Acetonitrile-Sodium Acetate Buffer, Ph 5 (60:40); FR: 1.4 Ml·Min−1; Column: XTERRA® MS C18 (250 Mm × 4.6 Mm) With 5 µm Particles; T R: 7.751 Min; Temperature: 25°C; UV Detection (275 Nm)	[43]
LC–MS	Pharm. Prep.	Solvent: Methanol; MP: Acetonitrile And 20 Mm Ammonium Acetate Solution (5:1), Ph 7.4; FR: 1 Ml·Min−1; Column: Shimpack GLC-CN (150 Mm × 4 Mm) With 5 µm Particles; T R: <5 Min; Vaporization Temperature: 200°C; Detection: M/Z 355.8; APCI; Negative Ion Mode; 430–450°C	[44]
LC–MS/MS	Rabbit Plasma And Uterine Tissue	Solvent: Methanol; MP: Methanol–Acetonitrile–Water–Formic Acid (45:45:10:0.5); FR: 0.5 Ml·Min−1; Column: Diamonsil C18 (150 Mm × 4.6 Mm) With A Phenomenax C18 Guard Cartridge (4 Mm × 3 Mm), Both With 5 µm Particles; Temperature: 20°C; Detection: M/Z 358 →→ 111; APCI; Positive Ion Mode; 450°C	[45]
LC–MS/MS	Rat Plasma	Solvent: Methanol; MP: Formic Acid–Acetonitrile (25:75); FR: 0.6 Ml·Min−1; Column: Atlantis Dc18 Column (50 Mm × 4.6 Mm) With 3 µm Particles; T R: 1.79 Min; Room Temperature; Detection: M/Z 357.7 →→ 139.1; ESI; Positive Ion Mode; 400°C	[46]
LC–MS/MS	Human Plasma And Urine	Solvent: Methanol; MP: Formic Acid–Acetonitrile (47:53); FR:1 Ml·Min−1; Column: Waters Symmetry C18 Column (150 Mm × 4.6 Mm) With 5 µm Particles Fitted With A Phenomenex C18 Guard Column (4 Mm × 3 Mm); T R: 8.6 Min; Detection: M/Z 358 →→ 139; ESI; Positive Ion Mode; 200°C	[47]
MEKC	Human Plasma	Carrier: Tris Buffer, Ph 8 With Sodium Octanesulfonate; Uncoated Fused-Silica Capillary (312 Mm × 0.075 Mm); Separation Voltage: 10 Kv; Temperature: 25°C; UV Detection (254 Nm, Cathode At The Detection Side), µ E: −1.76 × 10−4 Cm2·V−1·S−1; Migration Time: 5.94 Min	[48]
DPV	Pharm. Prep	Solvent: Acetonitrile; Working HMDE (0.4 Mm^2); Reference Electrode: Ag/Agcl; Auxiliary Electrode: Platinum Wire; Potential Range: −0.903 To −1.6 V; Scan Rate: 10 $Mv \cdot S^{-1}$; Pulse Amplitude: −50 Mv; Pulse Time: 40 Ms	[49]
DPV	Pharm. Prep. And Human Plasma	Solvent: Water; Working MWCNT–IL Modified Carbon Ceramic Electrode, Reference Electrode: Saturated Calomel; Auxiliary Electrode: Platinum Wire; Potential Range: 0–0.9 V; Scan Rate: 50 $Mv \cdot S^{-1}$	[50]

DPV	Pharm. Prep. And Human Plasma	Solvent: Water; Working MWCNT–IL Modified Carbon Ceramic Electrode, Reference Electrode: Saturated Calomel; Auxiliary Electrode: Platinum Wire; Potential Range: 0–0.9 V; Scan Rate: 50 $Mv \cdot S^{-1}$	[51]
SWV	Pharm. Prep., Human Urine And Blood Plasma	Solvent: Water; Working GCE Modified With Gold Nanorods-Graphene Oxide Nanocomposite Incorporated Carbon Nanotube Paste; Reference Electrode: Ag/Agcl; Auxiliary Electrode: Platinum Wire; Potential Range: 0.2–0.9 V; Scan Rate: 100 $Mv \cdot S^{-1}$; Pulse Amplitude: −50 Mv; Pulse Time: 40 Ms	[52]
DPV	Pharm. Prep., Human Urine And Blood Serum	Solvent: Water With Alkali; Working GCE Modified With Mwcnts; Reference Electrode: Ag/Agcl; Auxiliary Electrode: Platinum Wire; Potential Range: 0.2–1.4 V; Scan Rate: 50 $Mv \cdot S^{-1}$	[53]
DPV	Human Urine And Blood Serum	Solvent: Phosphate Buffer (0.1 M); Working GCE Modified With Mwcnts, Nhnps, And MCM-41 Molecular Sieve; Reference Electrode: Ag/Agcl; Auxiliary Electrode: Platinum Wire; Potential Range: −0.1–0.9 V; Scan Rate: 10–100 $Mv \cdot S^{-1}$	[54]
DPV	Human Urine And Blood Serum	Solvent: Phosphate Buffer (0.1 M); Working Gold Electrode Modified With Cdsnps And Mwcnts; Reference Electrode: Ag/Agcl; Auxiliary Electrode: —; Potential Range: 0–0.8 V; Scan Rate: 180–600 $Mv \cdot S^{-1}$	[55]
DPV	Pharm. Prep.	Solvent: Water; Working GCE Modified With Gr-Nio; Reference Electrode: Saturated Calomel; Auxiliary Electrode: Platinum Wire; Potential Range: 0.6–1.1 V; Scan Rate: 100 $Mv \cdot S^{-1}$; Amplitude: 0.05 V; Pulse Width: 0.05 S; Pulse Period: 0.5 S	[56]
Differential pulse polarography2	Rat Plasma	Solvent: Methanol And Dimethyl Formamide; Working HMDE (9 Mm^2); Reference Electrode: Ag/Agcl; Auxiliary Electrode: Platinum Wire; Potential Range: From 0 To −1.6 V; Scan Rate: 59.5 $Mv \cdot S^{-1}$; Pulse Amplitude: 0.1 V; Pulse Time: 0.01 S	[57]
DPV	Human Plasma	Solvent: Water With Alkali; Working Carbon Ionic Liquid Electrode Modified With Tio_2 Nanoparticles; Reference Electrode: Ag/Agcl; Auxiliary Electrode: Platinum Wire; Potential Range: 0–1 V; Scan Rate: 100 $Mv \cdot S^{-1}$	[58]
DPV	Pharm. Prep.	Solvent: Methanol; Working Boron-Doped Diamond Electrode; Reference Electrode: Ag/Agcl; Auxiliary Electrode: Platinum Plate; Potential Range: −0.5–1.3 V; Scan Rate: 10 $Mv \cdot S^{-1}$; Pulse Amplitude: 50 Mv; Pulse Time: 20 Ms; Potential Step: 5 Mv	[59]
Potentiometry	Pure Mixture Of	Solvent: Acetonitrile; ISE: Glass Electrode;	[60]

	Drugs	Reference Electrode: Ag/Agcl	
Potentiometry	Pharm. Prep.	Solvent: Ethanol; ISE: Liquid Membrane (Ion-Pair: Rhodamine B-INDO; Plasticizer: Dibutyl Phthalate; PVC; Solvent: Cyclohexanone); Reference Electrode: Ag/Agcl; Slope: 60 Mv·Decade^{-1}; Response Time: 3–5 S	[61]
Potentiometry	Pharm. Prep.	ISE: Liquid Membrane (Ion-Pair: Tetraethylammonium 1-(*P*-Chlorobenzyl)5-Methoxy-2-Methyl-3-Indolylacetate; Plasticizer: Dibutyl Phthalate; PVC; Solvent: Tetrahydrofuran); Reference Electrode: Ag/Agcl; Slope: 59.8 Mv·Decade^{-1}; Response Time: 12 S	[62]
ELISA	Water	Solvent: Methanol; Conjugate Preparation: Anhydride Ester Method; Conjugate: Goat Anti-Rabbit Igg-Horseradish Peroxidase; Absorption: 450 Nm	[63]
ELISA	Human Serum	Conjugates: INDO-Keyhole Limpet Hemocyanin; INDO-Ovalbumin, INDO-Horseradish Peroxidase; Conjugate Preparation: *N*-Hydroxysuccinimide Active Ester Procedure; Absorption: 450 Nm	[64]

5. Statistical Representation of Distribution of Analytical Methods For Indomethacin Determination

5.1.1 CHART I

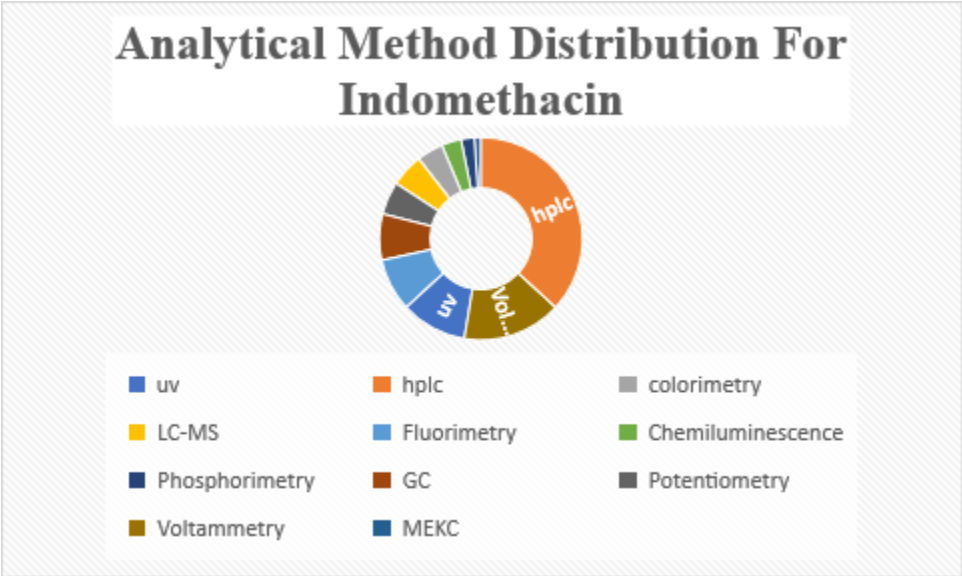

5.1.2 CHART II

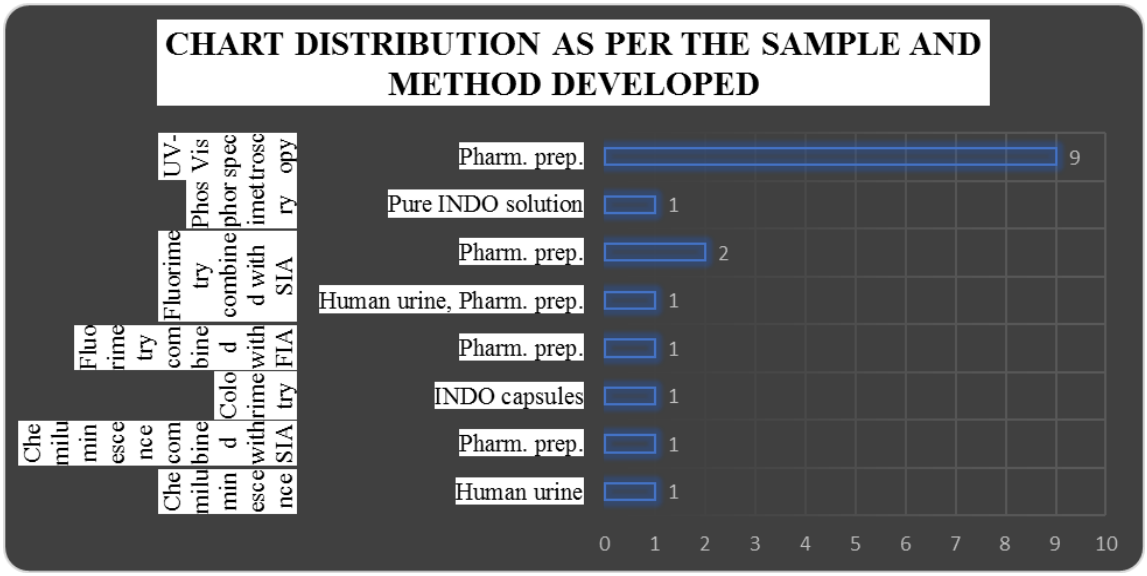

CONCLUION

In conclusion, this article provides a thorough exploration of Indomethacin, shedding light on its history, structure, how it works in the body, and its potential side effects. It discussed the binding affinity of indomethacin towards active site of protein and also discusses the various methods scientists use to measure Indomethacin. This information is valuable for researchers and healthcare professionals.

REFERENCES

1. Gliszczyńska A, Nowaczyk M. Lipid Formulations and Bioconjugation Strategies for Indomethacin Therapeutic Advances. Molecules, 2021 Mar 12; 26(6).
2. Villar-Martínez MD, Moreno-Ajona D, Chan C, Goadsby PJ. Indomethacin-responsive headaches-A narrative review. Headache, 2021 May; 61(5): 700-714.
3. Tripathi, K.D. (2015) *Essentials of Medical Pharmacology*. New Delhi: Jaypee Brothers Medical Publishers (P) Ltd.
4. Dandić, A. *et al.* (2022) 'Review of characteristics and analytical methods for determination of indomethacin', *Reviews in Analytical Chemistry*, 41(1): 34–62. doi: 10.1515/revac-2022-0032.
5. O'Brien M, McCauley J, Cohen E. Indomethacin. In Analytical profiles of drug substances 1984 Jan 1 (Vol. 13, pp. 211-238). Academic Press.
6. Dougherty C. Indomethacin-Induced Headache: Causing the Problem You Are Trying to Solve. Curr Pain Headache Rep, 2021 Nov 11; 25(11): 72.

7. LiverTox: Clinical and Research Information on Drug-Induced Liver Injury [Internet]. National Institute of Diabetes and Digestive and Kidney Diseases; Bethesda (MD): Mar 23, 2018. Indomethacin.
8. Kowalski ML, Makowska J. Use of nonsteroidal anti-inflammatory drugs in patients with aspirin hypersensitivity: safety of cyclo-oxygenase-2 inhibitors. Treat Respir Med, 2006; 5(6): 399-406.
9. Adegoke OA, Idowu OS, Olaniyi AA. Novel colorimetric assay of indomethacin using 4-carboxyl-2, 6-dinitrobenzene diazonium ion. Acta Pharmaceutica, 2006 Jun 1; 56(2): 189-202.
10. Nagaraja P, Vasantha RA, Yathirajan HS. Sensitive spectrophotometric method for the determination of indomethacin in capsules. Journal of pharmaceutical and biomedical analysis, 2003 Mar 10; 31(3): 563-9.
11. Stolarczyk M, Krzek J, Rzeszutko W. Application of derivative spectrophotometry to simultaneous determination of indomethacin and 5-methoxy-2-methyl-3-indoleacetic acid in metindol injections. J AOAC Int, 2004; 87(3): 592–5.
12. Maheshwari RK, Rathore A, Agrawal A, Gupta MA. New spectrophotometric estimation of indomethacin capsules with niacinamide as hydrotropic solubilizing agent. Pharm Methods, 2011; 2(3): 184–8.
13. Ali KF, Albakaa RM, Ali ZH. New assay method UV spectroscopy for determination of Indomethacin in pharmaceutical formulation. Journal of Chemical and Pharmaceutical Research, 2015; 7(4): 1591-6.
14. Rathod SB, Salunke PB, Kulkarni VC, Chavhan BR, Barhate SD. Spectroscopic quantitation and analytical validation of indomethacin in bulk drug and capsule formulation. J Pharm Res, 2017; 11(2): 124–7.
15. Jain S, Maheshwari R, Nema RK, Singhvi I. Development and validation of simple UV-spectrophotometric method of quantization of indomethacin in solid dosage formulation using mixed solvency concept. Pharma Innov J, 2017; 6(12): 453–6.
16. Rathod SB, Salunke PA, Kulkarni VC, Chavhan BR, Barhate SD. Method development and validation of indomethacin in bulk drug and capsule formulation by using mix hydrotrophy. Res J Pharm Dos Forms Technol, 2018; 10(3): 175.
17. Thejomoorthy K, Padma A, Snehith B, Raghu S, Siddhartha KS. A validated UV spectroscopic method development for estimation of indomethacin in bulk and its formulation. Glob J Res Anal, 2019; 8(1): 238–40.

18. Abed NK, Albakaa ARM, Ameen DSM, Jabbar ZA, Younis AS. Development of a novel method for quantitative determination of indomethacin. Int J Drug Deliv Technol, 2020; 10(1): 46–51.
19. Pinto PCAG, Saraiva MLMFS, Santos JLM, Lima JLFC. A pulsed sequential injection analysis flow system for the fluorimetric determination of indomethacin in pharmaceutical preparations. Anal Chim Acta, 2005; 539(1–2): 173–9.
20. Molina-García L, Fernández-De Córdova ML, Ruiz-Medina A. Sensitive determination of indomethacin in pharmaceuticals and urine by sequential injection analysis and optosensing. J AOAC Int, 2010; 93(5): 1443–9.
21. Passos MLC, Saraiva MLMFS, Santos JLM, Reis S, Lúcio M, Lima JLFC. A reagent-free method based on a photo-induced fluorimetry in a sequential injection system. Talanta, 2011; 84(5): 1309–13.
22. Turkie PNS, Alrazack HFA. Newly developed method for determination indomethacin using phosphotungstic acid by continue flow injection analysis via homemade ISNAG-fluorimeter. IOSR. J Appl Chem, 2018; 11(2): 25–39.
23. Kitade T, Kitamura K, Takegami S, Yoshinaga R, Sasakawa M, Tokuhira A. Determination of indomethacin by room-temperature phosphorimetry on a poly(vinyl alcohol) substrate. Anal Sci, 2002; 18(7): 835–8.
24. Nie F, Lu J, He Y, Du J. Determination of indomethacin in urine using molecule imprinting- chemiluminescence method. Talanta, 2005; 66(3): 728–33. 10.1016/j.talanta.2004.12.023.
25. Mervartová K, Polášek M, Calatayud JM. Sequential injection analysis (SIA)-chemiluminescence determination of indomethacin using tris[(2,2′-bipyridyl)]ruthenium(III) as reagent and its application to semisolid pharmaceutical dosage forms. Anal Chim Acta, 2007; 600(1–2 SPEC. ISS.): 114–21. 10.1016/j.aca.2007.01.057.
26. Hallaj T, Amjadi M, Manzoori JL, Azizi N. A novel chemiluminescence sensor for the determination of indomethacin based on sulfur and nitrogen co-doped carbon quantum dot–KMnO4 reaction. Luminescence, 2017; 32(7): 1174–9. 10.1002/bio.3306.
27. Thomas S, Sutton A, Garg U. Quantitation of indomethacin in serum and plasma using gas chromatography-mass spectrometry (GC-MS). Methods Mol Biol, 2010; 603: 297–305. 10.1007/978-1-60761-459-3_28.
28. Grippa E, Santini L, Castellano G, Gatto MT, Leone MG, Saso L. Simultaneous determination of hydrocortisone, dexamethasone, indomethacin, phenylbutazone and

oxyphenbutazone in equine serum by high-performance liquid chromatography. J Chromatogr B Biomed Sci Appl, 2000; 738(1): 17–25. 10.1016/S0378-4347(99)00478-8.

29. Nováková L, Matysová L, Havlíková L, Solich P. Development and validation of HPLC method for determination of indomethacin and its two degradation products in topical gel. J Pharm Biomed Anal, 2005; 37(5): 899–905. 10.1016/j.jpba.2004.09.012.
30. Boon V, Glass B, Nimmo A. High-performance liquid chromatographic assay of indomethacin in porcine plasma with applicability to human levels. J Chromatogr Sci, 2006; 44(1): 41–4. 10.1093/chromsci/44.1.41.
31. Al Za'abi MA, Dehghanzadeh GH, Norris RLG, Charles BG. A rapid and sensitive microscale HPLC method for the determination of indomethacin in plasma of premature neonates with patent ductus arteriousus. J Chromatogr B Anal Technol Biomed Life Sci, 2006; 830(2): 364–7. 10.1016/j.jchromb.2005.11.025.
32. Zhang Y, Zhang Z, Qi G, Sun Y, Wei Y, Ma H. Detection of indomethacin by high-performance liquid chromatography with in situ electrogenerated Mn(III) chemiluminescence detection. Anal Chim Acta, 2007; 582(2): 229–34.
33. Dawidowicz AL, Kondziola K, Kobielski M. Determination of free indomethacin in human plasma using HPLC with UV detection. J Liq Chromatogr Relat Technol, 2009; 32(18): 2686–98. 10.1080/10826070903245748.
34. Tsvetkova B, Pencheva I, Zlatkov A, Peikov P. High performance liquid chromatographic assay of indomethacin and its related substances in tablet dosage forms. Int J Pharm Pharm Sci, 2012; 4(3): 549–52.
35. Ivanov KV, Lukanov LK, Petrov G. Simultaneous HPLC determination of paracetamol and indomethacin in tablet dosage forms. Der Pharm Sin, 2013; 4(1): 102–5.
36. Nandy BC, Gupta AK, Mazumder B. Development and validation of analytical methods of indomethacin in rabbit blood plasma by RP-HPLC technique. J Biomed Pharm Res, 2013; 2(5): 1–6.
37. Haq N, Shakeel F, Ali M, Elbadry M, Alanazi FK, Alsarra IA. An environmentally benign approach for rapid analysis of indomethacin using a stability-indicating RP-HPLC method. J Liq Chromatogr Relat Technol, 2014; 37(6): 878–92. 10.1080/10826076.2012.758150.
38. Lariya NK, Agrawal GP. Development and validation of RP-HPLC method for simultaneous determination of methotrexate, dexamethasone and indomethacin. Int J Pharm Pharm Sci., 2014; 7(3): 443–6.

39. Babu GR, Rao AL, Rao JV. Bioanalytical method development and validation for the simultaneous estimation of indomethacin and omeprazole in rabbit plasma by using HPLC. Int J Chem Sci., 2016; 14(2): 585–94.
40. Chamkouri N, Zare-Shahabadi V, Niazi A. Ultrasound-assisted dispersive liquid-liquid microextraction with HPLC-UV for the simultaneous determination of diclofenac potassium and indomethacin in serum and plasma samples: experimental design and optimization. Bulg Chem Commun., 2017; 49(4): 994–1000.
41. Elshorbagy NH, Ali K, Farghaly U, Ali F, Elgarhy O. Analytical assay of indomethacin in presence of quercetin for indomethacin induced peptic ulcer prevention. Malaysian J Med Res., 2017; 28(2): 267–71.
42. Pai S, Sawant N. Applications of new validated RP-HPLC method for determination of indomethacin and its hydrolytic degradants using sodium acetate buffer. Indian J Pharm Educ Res., 2017; 51(3): 388–92. 10.5530/ijper.51.3.65.
43. Assali M, Abualhasan M, Zohud N, Ghazal N. RP-HPLC method development and validation of synthesized codrug in combination with indomethacin, paracetamol, and famotidine. Int J Anal Chem., 2020; 2020: 1894907. 10.1155/2020/1894907. Search in Google Scholar
44. Abdel-Hamid ME, Novotny L, Hamza H. Determination of diclofenac sodium, flufenamic acid, indomethacin and ketoprofen by LC-APCI-MS. J Pharm Biomed Anal. 2001; 24(4): 587–94. 10.1016/S0731-7085(00)00444-1.
45. Liu Y, Guan F, Wang X, Zhang X, Di X. Development of a liquid chromatography-tandem mass spectrometry method for measuring plasma and uterine tissue levels of indomethacin in rabbits treated with indomethacin-medicated Cu-IUDs. Contraception. 2012; 85(4): 419–24. 10.1016/j.contraception.2011.08.018.
46. Suresh PS, Dixit A, Giri S, Rajagopal S, Mullangi R. Development and validation of a liquid chromatography-tandem mass spectrometry method for quantitation of indomethacin in rat plasma and its application to a pharmacokinetic study in rats. Biomed Chromatogr. 2013; 27(4): 496–501. 10.1002/bmc.2818.
47. Wang X, Vernikovskaya DI, Nanovskaya TN, Rytting E, Hankins GDV, Ahmed MS. A liquid chromatography method with single quadrupole mass spectrometry for quantitative determination of indomethacin in maternal plasma and urine of pregnant patients. J Pharm Biomed Anal. 2013; 78–79: 123–8. 10.1016/j.jpba.2013.02.006.
48. Lin SJ, Chen YR, Su YH, Tseng HI, Chen SH. Determination of indomethacin in plasma by micellar electrokinetic chromatography with UV detection for premature infants with

patent ducts arteriosus. J Chromatogr B Anal Technol Biomed Life Sci., 2006; 830(2): 306–13. 10.1016/j.jchromb.2005.11.007.

49. Reguera C, Ortiz MC, Arcos MJ. Differential pulse voltammetric simultaneous determination of four anti-inflammatory drugs by using soft modelling. Electroanalysis, 2002; 14(24): 1699–706. 10.1002/elan.200290013.
50. Sarhangzadeh K, Mmohamma-Rezaei R, Jabbri M. Room-temperature ionic liquid and multi-walled carbon nanotube composite modified carbon-ceramic electrode as a sensitive voltammetric sensor for indomethacin. Anal Lett., 2014; 47(1): 134–45. 10.1080/00032719.2013.832267.
51. Sarhangzadeh K, Khatami AA, Jabbari M, Bahari S. Simultaneous determination of diclofenac and indomethacin using a sensitive electrochemical sensor based on multiwalled carbon nanotube and ionic liquid nanocomposite. J Appl Electrochem, 2013; 43(12): 1217–24. 10.1007/s10800-013-0609-3.
52. Arvand M, Gholizadeh TM. Gold nanorods-graphene oxide nanocomposite incorporated carbon nanotube paste modified glassy carbon electrode for voltammetric determination of indomethacin. Sens Actuators, B Chem., 2013; 186: 622–32. 10.1016/j.snb.2013.06.059.
53. Sataraddi SR, Patil SM, Bagoji AM, Pattar VP, Nandibewoor ST. Electrooxidation of indomethacin at multiwalled carbon nanotubes-modified GCE and its determination in pharmaceutical dosage form and human biological fluids. ISRN Anal Chem., 2014; 2014: 1–9. 10.1155/2014/816012.
54. Babaei A, Yousefi A, Afrasiabi M, Shabanian M. A sensitive simultaneous determination of dopamine, acetaminophen and indomethacin on a glassy carbon electrode coated with a new composite of MCM-41 molecular sieve/nickel hydroxide nanoparticles/multiwalled carbon nanotubes. J Electroanal Chem., 2015; 740: 28–36. 10.1016/j.jelechem.2014.12.042.
55. Babaei A, Yousefi A. A Sensitive simultaneous determination of uric acid, norepinephrine and indomethacin using a cadmium sulfide nanoparticles/multi-walled carbon nanotubes modified gold electrode. Anal Bioanal Electrochem. 2020; 12(4): 486–501.
56. Liu Y, Huang Q, Zhang C, Liang C, Wei L, Peng J. A novel method for indomethacin determination based on graphene loaded nickel oxides nanoparticles film. Int J Electrochem Sci., 2018; 13(2): 1484–94. 10.20964/2018.02.39.

57. Ragab MAA, Korany MA, Galal SM, Ahmed AR. Voltammetric analysis of dantrolene and its active metabolite with indomethacin in rat plasma. Bioanalysis, 2019; 11(2): 73–84. 10.4155/bio-2018-0165.
58. Baezzat MR, Banavand F, Kamran Hakkani S. Sensitive voltammetric detection of indomethacin using TiO2 nanoparticle modified carbon ionic liquid electrode. Anal Bioanal Chem Res., 2020; 7(1): 89–98. 10.22036/ABCR.2019.171887.1317.
59. Petković BB, Ognjanović M, Krstić M, Stanković V, Babincev L, Pergal M, et al. Boron-doped diamond electrode as efficient sensing platform for simultaneous quantification of mefenamic acid and indomethacin. Diam Relat Mater., 2020; 105: 107785. 10.1016/j.diamond.2020.107785.
60. Aktaş AH, Ertokuş GP. Potentiometric determination of ibuprofen, indomethacin and naproxen using an artificial neural network calibration. J Serbian Chem Soc., 2008; 73(1): 87–95. 10.2298/JSC0801087A.
61. Kormosh Z, Hunka I, Bazel Y. Potentiometric sensor for the indomethacin determination. Mater Sci Eng C., 2009; 29(3): 1018–22. 10.1016/j.msec.2008.09.003.
62. Lenik J, Wardak C. Characteristic of a new sensor for indomethacin determination. Procedia Eng., 2012; 47: 144–7. 10.1016/j.proeng.2012.09.105.
63. Huo SM, Yang H, Deng AP. Development and validation of a highly sensitive ELISA for the determination of pharmaceutical indomethacin in water samples. Talanta, 2007; 73(2): 380–6. 10.1016/j.talanta.2007.03.055.
64. Skalka N, Krol A, Schlesinger H, Altstein M. Monitoring of the non-steroid anti-inflammatory drug indomethacin: development of immunochemical methods for its purification and detection. Anal Bioanal Chem., 2011; 400(10): 3491–504. 10.1007/s00216-011-5027-y.
65. L. Chen *et al.*, "Inflammatory responses and inflammation-associated diseases in organs.," *Oncotarget*, Jan. 2018; 9(6): 7204–7218, doi: 10.18632/oncotarget.23208.
66. Magedov IV, Maklakov SA, Smushkevich YI. New procedure for obtaining indomethacin. Chem Heterocycl Compd.
67. L. Chen *et al.*, "Inflammatory responses and inflammation-associated diseases in organs.," *Oncotarget*, Jan. 2018; 9(6): 7204–7218, doi: 10.18632/oncotarget.23208.
68. R. G. Kurumbail *et al.*, "Structural basis for selective inhibition of cyclooxygenase-2 by anti-inflammatory agents," *Nature*, Dec. 1996; 384(6610): 644–648, doi: 10.1038/384644a0.
69. R. G., S. A. M., G. J. K., M. J. J., S. R. A., P. J. Y., G. D., M. J. M., P. T. D., S. K., I. P.

C., S. W. C. Kurumbail, "Structural basis for selective inhibition of cyclooxygenase-2 by anti-inflammatory agents.," 1996.

70. J. L. Wang *et al.*, "The novel benzopyran class of selective cyclooxygenase-2 inhibitors. Part 2: The second clinical candidate having a shorter and favorable human half-life," *Bioorg Med Chem Lett*, Dec. 2010; 20(23): 7159–7163, doi: 10.1016/j.bmcl.2010.07.054.
71. K. C. Duggan *et al.*, "Molecular basis for cyclooxygenase inhibition by the non-steroidal anti-inflammatory drug naproxen," *Journal of Biological Chemistry*, Nov. 2010; 285(45): 34950–34959, doi: 10.1074/jbc.M110.162982.
72. B. J. Orlando and M. G. Malkowski, "Crystal structure of rofecoxib bound to human cyclooxygenase-2," *Acta Crystallographica Section: F Structural Biology Communications*, Oct. 2016; 72(10): 772–776, doi: 10.1107/S2053230X16014230.
73. S. Sharma, S. Sharma, V. Pathak, P. Kaur, and R. K. Singh, "Drug Repurposing Using Similarity-based Target Prediction, Docking Studies and Scaffold Hopping of Lefamulin," *Lett Drug Des Discov*, Sep. 2021; 18(7): 733–743, doi: 10.2174/1570180817999201201113712.
74. B. O. Moreira *et al.*, "New dimer and trimer of chalcone derivatives from anti-inflammatory and antinociceptive extracts of Schinopsis brasiliensis roots," *J Ethnopharmacol*, May 2022; 289: 115089, doi: 10.1016/j.jep.2022.115089.
75. G. M. Morris *et al.*, "AutoDock4 and AutoDockTools4: Automated docking with selective receptor flexibility.," *J Comput Chem*, Dec. 2009; 30(16): 2785–91, doi: 10.1002/jcc.21256.
76. N. Kumar, N. Goel, T. Chand Yadav, and V. Pruthi, "Quantum chemical, ADMET and molecular docking studies of ferulic acid amide derivatives with a novel anticancer drug target," *Medicinal Chemistry Research*, Aug. 2017; 26(8): 1822–1834, doi: 10.1007/s00044-017-1893-y.
77. N. Razzaghi-Asl, S. Mirzayi, K. Mahnam, and S. Sepehri, "Identification of COX-2 inhibitors via structure-based virtual screening and molecular dynamics simulation," *J Mol Graph Model*, Aug. 2018; 83: 138–152, doi: 10.1016/j.jmgm.2018.05.010.
78. C. A. Lipinski, "Drug-like properties and the causes of poor solubility and poor permeability," *J Pharmacol Toxicol Methods*, Jul. 2000; 44(1): 235–249, doi: 10.1016/S1056-8719(00)00107-6.
79. K. E. Hevener *et al.*, "Validation of Molecular Docking Programs for Virtual Screening against Dihydropteroate Synthase," *J Chem Inf Model*, Feb. 2009; 49(2): 444–460, doi: 10.1021/ci800293n.

80. J. Cruz *et al.*, "Identification of Novel Protein Kinase Receptor Type 2 Inhibitors Using Pharmacophore and Structure-Based Virtual Screening," *Molecules*, Feb. 2018; 23(2): 453, doi: 10.3390/molecules23020453.
81. I. V. F. Dos Santos *et al.*, "Hierarchical Virtual Screening Based on Rocaglamide Derivatives to Discover New Potential Anti-Skin Cancer Agents.," *Front Mol Biosci*, 2022; 9: 836572, doi: 10.3389/fmolb.2022.836572.
82. A. P. Li, "Screening for human ADME/Tox drug properties in drug discovery," *Drug Discov Today*, Apr. 2001; 6(7): 357–366, doi: 10.1016/S1359-6446(01)01712-3.
83. N. Razzaghi-Asl, S. Mirzayi, K. Mahnam, and S. Sepehri, "Identification of COX-2 inhibitors via structure-based virtual screening and molecular dynamics simulation," *J Mol Graph Model*, Aug. 2018; 83: 138–152, doi: 10.1016/j.jmgm.2018.05.010.
84. Alagga AA, Gupta V. Drug Absorption. [Updated 2023 Jun 20]. In: StatPearls [Internet]. Treasure Island (FL): StatPearls Publishing; 2023 Jan-. Available from: https: //www.ncbi.nlm.nih.gov/books/NBK557405/